Power Resilient, Air-Gap Multi-Core Fiber with >20 W Fiber Fuse Propagation Threshold per Core

Aditi Mehta[1], Kazunori Mukasa[2], Takeshi Takagi[3], Mujtaba Zahidy[1], Yaoxin Liu[1], Kjeld Dalgaard[1], Karsten Rottwitt[1], Michael Galili[1], Leif Katsuo Oxenløwe[1], and Toshio Morioka[1]

1. Technical University of Denmark, Department of Electrical and Photonics Engineering, 2800 Kgs. Lyngby, Denmark
2. Furukawa Electric Co., Ltd, Telecommunications & Energy Laboratories, 20-16, Nobono, Kameyama, Mie, 519-0292, Japan
3. Furukawa Electric Co., Ltd, Telecommunications & Energy Laboratories, 6, Yawata-Kaigandori, Ichihara, Chiba, 290-855, Japan
e-mail; adime@dtu.dk

Abstract: We measured fiber fuse properties of FMFs, coupled/uncoupled MCFs, and novel air-gap MCFs. We found that air-gap MCFs have fiber fuse propagation threshold of more than 20 W owing to efficient heat diffusion into air.

1. Introduction

Space-division multiplexing (SDM) has become crucial in solving the problem of capacity crunch [1]. Researchers have been exploring SDM fibers, such as few-mode fibers (FMFs) [2], single-mode (SM) uncoupled/coupled-core multi-core fibers (UC/CC MCFs) [3,4,5], and FM-MCFs [6,7] as potential high-capacity data transmission channels. With advancements in the fabrication of novel SDM fibers [8] and supporting technologies such as micro-comb sources [9], research towards 100 Pbit/s transmission is underway. However, transmitting more bits through a fiber means sending more optical power through fibers added even by Raman pump powers. There is also a growing need to use optical fibers for both transmitting data and feeding power simultaneously for remote antenna units and distributed sensors, which requires high optical powers to pass through the fibers [10]. Such high-power applications can make the fibers prone to fiber fuse (FF) [11]. Studies have examined the FF propagation threshold (stopping) powers (P_{th}) for conventional single-mode fibers (SMFs) and step-index few-mode fibers (SI-FMFs) to be 1.4 W and no more than 2 W, respectively [12, 13]. However, there have been no comprehensive studies of FF phenomena for SDM fibers. In this study, we examined FF phenomena in different SDM fibers, including a 4-mode graded-index (GI) FMF, a trenched-assisted SM 7-core UC-MCF, a 4-core CC-MCF and a novel 6-core SM air-gap (AG) UC-MCF [14]. The FF threshold powers slightly depended on the core position in the UC-MCF, while FF propagation stopped after some distances in the CC-MCF. We confirmed that the AG-MCF showed a high-power tolerance with FF propagation threshold power P_{th} of more than 20 W, suggesting that the air-gap structures should greatly improve FF resistance owing to its efficient heat diffusion into the air-gap.

2. Experimental Setup

The experimental setup for measuring the FF propagation threshold power P_{th} is shown in Fig.1(b) whereas the SDM fibers studied are shown in Fig. 1 (a). A high-power CW fiber laser (IPG ELR-AC, 100 W, 1567 nm, beam diameter 4.5 mm, unpolarized) was used to initiate FF in the fiber under test (FUT). The laser output was passed through a combination of the polarization beam splitters (PBSs) and half-wave plates (HWPs) to change the input optical powers and to ensure that the power can be lowered enough to safely couple light into the FUT without damaging its tip.

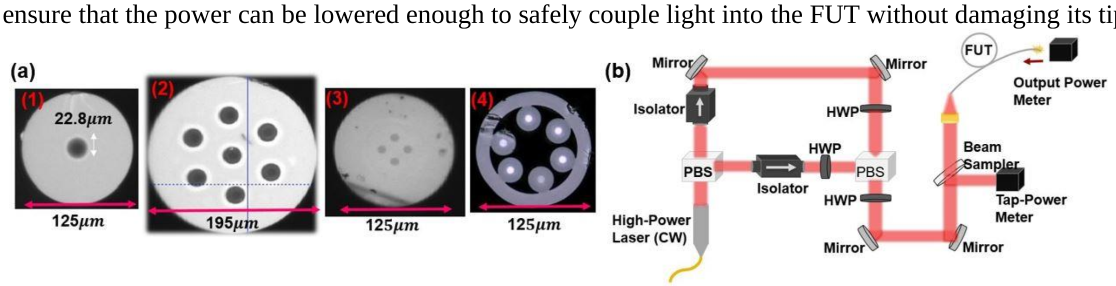

Fig.1. (a) SDM fibers used in the study: (1) GI-FMF, (2) 7-core SM UC-MCF, (3) 4-core CC-MCF, (4) 6-core SM AG UC-MCF, (b) experimental setup.

A beam sampler (1.6 %) is used to monitor the power coupled into the FUT. To calibrate the monitoring power meter and the output power meter, the HWPs are rotated over 45 degrees and the correlated powers were saved. To initiate FF at the output end of the FUT, an absorptive/reflective substance (such as a metal filer rod) was introduced at the end tip of the FUT. The FF propagation threshold powers were then measured by reducing the coupled optical power by rotating back the HWPs and measuring the power at which FF propagation ceased.

3. Results and Discussions

3.1 GI-FMF

Fig.2 (a) shows the images of the cross-section and side view of the GI-FMF taken using a Vytran glass processor. Cross-sectional views after and before FF propagation showed the effects on the initial core diameter of 22.8 μm, which expanded to a damaged region of diameter 30.6 μm (D_{melted} [13]) due to FF propagation. When launching a 2.3 W Gaussian beam into the FMF for FF initiation, a repetitive sequence of voids with a 266 μm period was observed. Unlike SMFs' bullet-shaped voids, these voids resulted from interference of multiple excited modes supported by the FMF [15]. See Fig.2 (a) images (1) and (2). Image (3) shows a slight change in the period of void sequence as input power reduced gradually from 2.3 W. Eventually, voids terminated and a round blob structure formed, representing the stopping point of FF, as seen in image (4). The experiment showed that the P_{th} for FF in FMF is mode-dependent with 1.3 W recorded as the minimum threshold in 8 out of 11 trials. The average speed of FF propagation was 43.5 cm/s. GI-FMF has a lower minimum threshold than SI-FMF (1.7 W) [13].

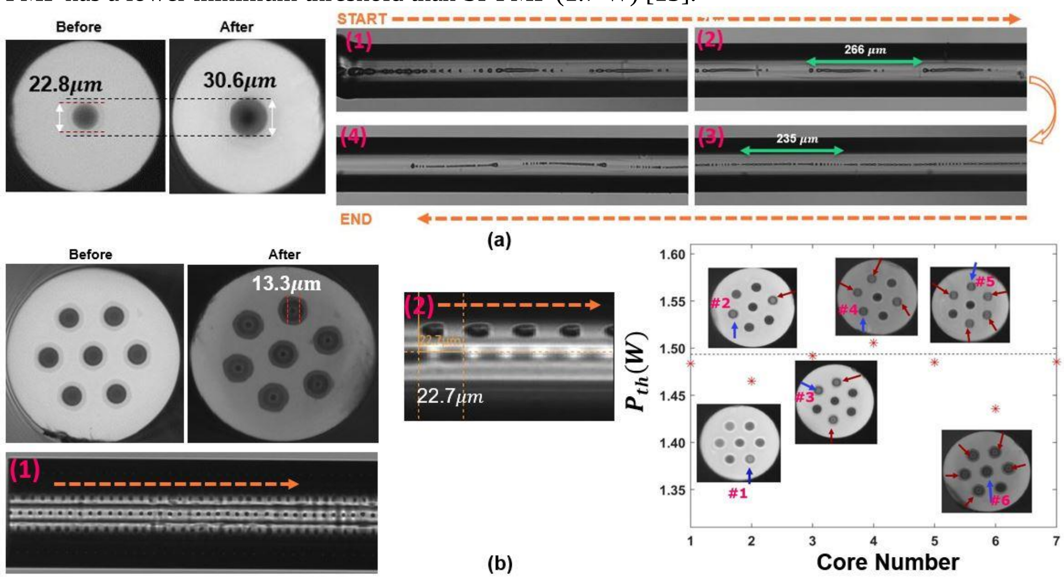

Fig. 2. (a) GI-FMF: cross-sectional views of before and after FF (left), side views after FF (middle and right), (b) 7-core SM UC-MCF: cross-sectional views before and after FF(top left), (1) side views after FF in all the cores, (2) bullet-shaped voids (middle), P_{th} of each of the 7 cores (right).

3.2 7-core SM UC-MCF

Around 3 W was coupled successively into each core of the MCF (MFD: 11.8 μm, core pitch: 49.8 μm, 100-km crosstalk (XT): -62.7 dB at 1550 nm). FF with very bright white light propagated toward the source with an average velocity of 35.2 cm/s. The cross-sectional views before and after FF are shown in the top left of Fig. 2 (b), which depict the damaged cores having D_{melted} around 13.3 μm. It was observed that the propagation of FF in one of the cores did not damage the other cores. P_{th} was measured as shown in the bottom right of Fig.2 (b). It was observed that the measured P_{th} was lower for the center core (1.44 W), which is core number 6, than for the outer cores (1.49 W av). Bullet-shaped voids were observed in Fig.2 (b) (1), having a period of around 22.7 μm as shown in the detail view (2).

3.3 4-Core CC-MCF

We struggled to initiate FF in CC-MCF (core diameter: 8.6 μm, core pitch: 19 μm) due to its complex coupling behavior. Although we observed slight propagation up to less than one cm of the fiber length at 6.6 W coupled power, all four cores were affected by FF, as seen in Fig.3(a). At 10 W input power, FF initiated again and formed different sized FF-voids around the four cores (Fig.3(b)). FF propagation stopped by itself in both cases, possibly due to the sharing of total launched power among the four cores, reducing the power density required for stable FF propagation.

3.4 6-Core SM AG UC-MCF

FF properties of a novel 6-core AG UC-MCF [14] was investigated as shown in Fig.3 (c). Maximum 20 W of power was coupled into one of the cores of this MCF, but no FF propagation was observed although the core dimension of the fiber is similar to that of a conventional SMF. At 18 W, the output end of the fiber melted as shown in Fig.3 (c) (2). In one of the trials, a tiny FF-void-like formation did appear at the coupled power of 4.7 W, but no FF-propagation happened as shown in Fig.3 (c) (3). The presence of air surrounding the cores acts as a heat diffusion channel and plasma energy build-up in the core during the initiation of FF would ooze out making the FF unstable for propagation inside the core as depicted in the bottom right figure of Fig. 3 (c). The higher thermal diffusivity of air than silica makes the AG MCF design >10 times more power tolerant per core than the conventional solid-cladding MCF design.

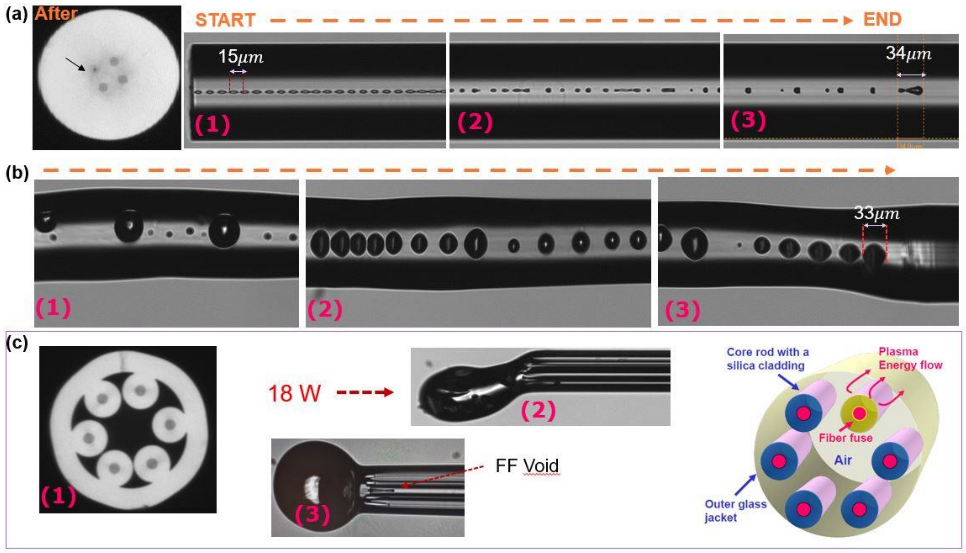

Fig.3. 4-core CC-MCF: (a) Cross sectional and side views of CC-MCF after FF propagation at 6.6 W, (b) side view of CC-MCF after FF propagation at 10 W. (c) 6-core AG UC-MCF: (1) cross sectional view, (2) side view showing the melted end at 18 W, (3) side view with a visible tiny FF voids, right bottom: schematic to depict the outward diffusive flow of plasma energy through air, which makes the FF propagation harder to sustain inside the core.

4. Conclusions

We experimentally confirmed that the existing SDM optical fibers such as FMF, and solid-cladding UC-MCF have low FF thresholds P_{th} of < 2W and are under a constant threat of FF-propagation for high-power applications. Moreover, the complex behavior of FF phenomena in a CC-MCF is reported. We found that the novel air-gap MCF can have a very high P_{th} of more than 20 W, making it a promising candidate for high-capacity/high-power transmission.

5. Acknowledgement

This study is supported by DNRF Research CoE SPOC (ref. DNRF123) and the Carlsberg Foundation (CF21-0644).

6. References

[1] M. Nakazawa, M. Suzuki, Y. Awaji and T. Morioka, (eds) "*Space-Division Multiplexing in Optical Communication Systems*" Springer Series in Optical Sciences, vol 236. Springer, Cham. https://doi.org/10.1007/978-3-030-87619-7 (2022).
[2] G. Rademacher et al. "3.56 Peta-bit/s C+L Band Transmission over a 55-mode Multi-Mode Fiber," COC 2023, We.A.1.1 (2023).
[3] H. Takara et al., "1.01-Pb/s (12 SDM/222 WDM/456 Gb/s) Crosstalk-managed Transmission with 91.4-b/s/Hz Aggregate Spectral Efficiency," ECOC 2012, Th.3.C.1 (2012).
[4] B. J. Puttnam et al., "1 Pb/s Transmission in a 125μm diameter 4-core MCF," CLEO 2022, JTh6B.1(2022).
[5] G. Rademacher et al., "Randomly Coupled 19-Core Multi-Core Fiber with Standard Cladding Diameter," OFC 2023, Th4A.4 (2023).
[6] D. Soma et al., "10.16 Peta-bit/s dense SDM/WDM transmission over low-DMD 6-mode 19-core fibre across C+L band," ECOC 2017, Th.PDP.A.1 (2017).
[7] B. J. Puttnam et al., "22.9 Pb/s Data-Rate by Extreme Space-Wavelength Multiplexing," ECOC 2023, Th.C.2.1 (2023).
[8] K. Mukasa, "Ultra-high-density uncoupled multi-core fibers", Next-Generation Optical Communication: Components, Sub-Systems, and Systems XI. Vol. 12028, 1202806, SPIE (2022).
[9] A. A. Jørgensen et al., "Petabit-per-second data transmission using a chip-scale microcomb ring resonator source," Nat. Photon. 16, 798–802 (2022).
[10] M. Wada et al., "High-Efficiency and Long-Distance Power-over-Fibre Transmission using a 125-μm Cladding Diameter 4-Core Fibre," ECOC 2023, We.D.7.5 (2023).
[11] S. Todoroki, "*Fiber Fuse*" NIMS series, Springer. https://doi.org/10.1007/978-4-431-54577-4 (2014).
[12] A. M. Rocha et al., "Threshold power of fiber fuse effect for different types of optical fiber," 2011 13th International Conference on Transparent Optical Networks. IEEE (2011).
[13] N. Hanzawa et al., "Fiber Fuse Propagation Characteristics of LP01 and LP11 Modes in Few-Mode Fiber," J. Lightwave Technol. 34, 3628-3632 (2016).
[14] K. Mukasa et al., "Uncoupled 6-core Fibers with a Standard 125-μm Cladding, ITU-T G. 652 Optical Properties, and Low XT," OFC 2023, M3B.2 (2023).
[15] S. Jiang et al., "Observation of fiber fuse propagation speed oscillation due to inter-mode interference in two-mode fibers," OFC 2018, Th2A.26 (2018).